JASMAC
Conference of the Japan Society of Microgravity Appllication

OR-0707

微小重力場大気圧雰囲気での液滴群要素の燃え広がりにおける冷炎発生の調査

Investigation of Occurrence of Cool Flame During Flame Spread over Droplet-cloud Elements at Atmospheric Pressure in Microgravity

松本昂大[1]，千頭勇斗[1]，瀬尾健彦[1]，三上真人[1]

Kodai MATSUMOTO[1], Yuto CHIKAMI[1], Takehiko SEO[1] and Masato MIKAMI[1]

1 山口大学大学院創成科学研究科，
Graduate School of Sciences and Technology for Innovation, Yamaguchi University

1. Introduction

Spray combustion is used in many combustors. However, its mechanism is complicated because the atomization of fuel, vaporization, mixing and chemical reaction progress simultaneously and has not been clarified completely. Although many studies on droplet combustion in microgravity have been carried out to elucidate the fundamental aspects of spray combustion, there is still a large gap in understanding between droplet combustion and spray combustion. Thus, in 2017, droplet-cloud combustion experiments titled “Elucidation of Flame Spread and Group Combustion Excitation Mechanism of Randomly Distributed Droplet Clouds (Group Combustion)” [1)] were conducted as the first combustion experiments in the Japanese Experimental Module Kibo aboard the International Space Station (ISS), in order to bridge the above mentioned gap. In “Group Combustion” experiments, flame spread experiments over droplet-cloud elements with strong droplet interaction [2)] and randomly distributed droplet clouds [3-5)] were respectively conducted to study the effects of droplet interaction on the flame spread and to study group-combustion-excitation characteristics in high-quality, long-duration microgravity aboard ISS. In the flame spread over a randomly distributed droplet cloud near the group-combustion-excitation limit, a large-scale ignition phenomenon in which multiple droplets are ignited at the same time was observed, which has not been seen in past experiments [4,5)]. Matsumoto et al. [6)] and Mikami et al. [7)] investigated the cause of occurrence of large-scale ignition based on the additional experiments aboard Kibo using droplet-cloud elements that consist of a few droplets simulating an important element of randomly distributed droplet clouds in "Group Combustion." They suggested that a cool flame may appear in the flame spread over droplets and contribute to the large-scale ignition.

This study investigated the occurrence of cool flame based on the vaporization-rate constant and temperature distribution for the same droplet arrangement that the cool flame is considered to have occurred in “Group Combustion.”

2. Experimental Apparatus and Method

Figure 1 shows the droplet-cloud elements used in the experiments. This study used four *n*-decane droplets: Droplets I, B, A and L as shown in Fig. 1. The droplet cluster of Droplets I, B and A is called Cluster H. We observed whether a cool flame occurs around Droplet L. While the position of each droplet was fixed of $S_{AL} = 9.5$ mm and $S_{IA} = S_{AB} = 4$ mm, we used five different initial droplet diameters, d_0=0.5, 0.475, 0.45, 0.425 and 0.4 mm.

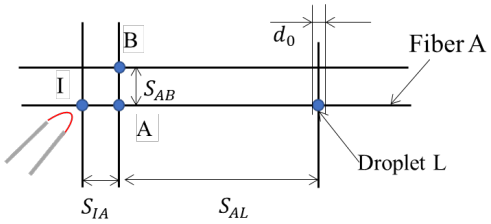

Fig. 1 Droplet-cloud element model.

Figure 2 shows the droplet supporting system, droplet-cloud element generator, and ignition system. The droplet supporting system has several 14-μm SiC fibers (Nippon Carbon, Hi-Nicalon) and droplets generated at intersections of Si-C fibers using the droplet-cloud element generator. This device generates droplets at the pre-determined intersections of Si-C fibers by supplying the fuel through a glass-tube needle. A certain amount of fuel is pushed out from a stepping-motor-driven syringe and is delivered to the glass-tube needle through a Teflon tube. The fuel-supply glass-tube needle is moved by a three-axis traverse system and the droplet is generated one by one. The ignition system starts the flame spread by ignition of Droplet I using electrically heated resistance wire.

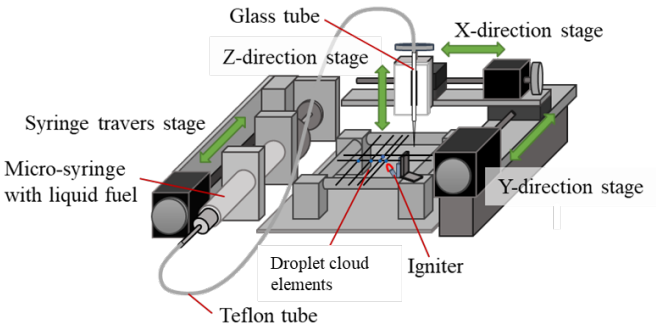

Fig. 2 Droplet-cloud element generation systems.

We investigated the vaporization characteristics of Droplet L and temperature distribution around Droplet L. To investigate the vaporization characteristics, we used a high-speed camera (IDT, iN8-S2) with 1000 fps with a back-light module and measured the diameter of Droplet L after the Cluster H ignition. In order to obtain the temperature distribution around Droplet L based on the Thin Filament Pyrometry (TFP), we used an infrared camera (Allied Vision, Goldeye G033 SWIR) with 160 ± 10 fps and measured the luminosity of SiC fibers. Figure 3 shows the calibration result of TFP method using the infrared camera. Since the brightness value is constant below about 700 K, accurate temperature measurement cannot be performed due to the influence of noise in such a low temperature range. All experiments were conducted at atmospheric pressure and room temperature. The microgravity experiments were performed at the drop experiment facility of Yamaguchi University, Japan, providing the microgravity duration time of 0.9 s.

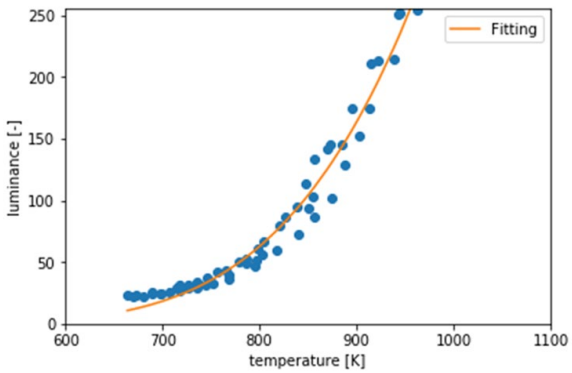

Fig. 3 Calibration result of relation between temperature and luminosity of SiC fiber using an infrared camera.

3.Results and Discussion

3.1 Vaporization of Droplet L for Different Initial Droplet Diameter

We calculated the vaporization-rate constant of Droplet L based on the temporal variation of the squared Droplet L diameter. Figure 4 shows the temporal variations of the squared Droplet L diameter after the start of burning of Cluster H. The horizontal axis is the normalized time $t/{d_0}^2$. $t/{d_0}^2 = 0$ s/mm² is the timing of ignition of Droplet I. The vertical axis is the dimensionless squared droplet diameter $(d/d_0)^2$, where d_0 is the initial diameter of Droplet L. In each condition, we calculated an approximate line while Droplet L gets decrease in diameter. Then, we got the vaporization-rate constant of Droplet L as the absolute value of slop of the approximate line. The droplet diameter became bigger than the initial condition just before the start of vaporization. This phenomenon is caused by thermal expansion of Droplet L.

For the initial droplet diameter of 0.5 mm and 0.475 mm, a hot flame was observed around Droplet L. The vaporization-rate constant is 0.66 mm²/s regardless of initial droplet diameter. For the initial droplet diameter of 0.45 mm or less, the hot flame was not observed around Droplet L and Droplet L did not completely vaporize within the microgravity duration. The vaporization-rate constant depends on the initial droplet diameter. It is 0.23 mm²/s for $d_0 = 0.45$ mm, 0.16 mm²/s for $d_0 = 0.425$ mm, and 0.04 mm²/s for $d_0 = 0.4$ mm was. Nayagam et al. [8-9] conducted combustion experiments of large single droplets aboard ISS and showed that the liquid hydrocarbon droplet of a few mm in initial diameter first vaporizes with a hot-flame, and then radiative extinction of the hot-flame occurs, but the droplet vaporization continues with a cool-flame, while the vaporization-rate constant with the cool-flame is about 0.35 to 0.40 mm²/s for *n*-decane droplets. The vaporization-rate constant of Droplet L is smaller than that in Ref. 9). Since the flame spread over droplets is different from the single droplet combustion in Ref. 9), it may not be good to simply compare the vaporization-rate constant of ours with that of Ref. 9). Next, we compare the vaporization-rate constant of Droplet L with our previous results for the flame spread over droplet-cloud elements conducted in "Group Combustion" [6]. Reference 6) and the present experiment have the same droplet arrangement and close value of S_{AL}/d_0, S_{AL}/d_0=19.6 in Ref. 6) and S_{AL}/d_0=21.1 for d_0=0.45 mm in this experiment. However, the initial droplet diameter d_0 in Ref. 6) is about 1 mm, which is greater than that in this experiment. The vaporization-rate constant of Droplet L in Ref. 6) is 0.30 mm²/s, which is greater than that of 0.23 mm²/s for this experiment for $d_0 = 0.45$ mm. Based on these discussions, we think that it is difficult to judge the occurrence of a cool flame only by the vaporization-rate constant.

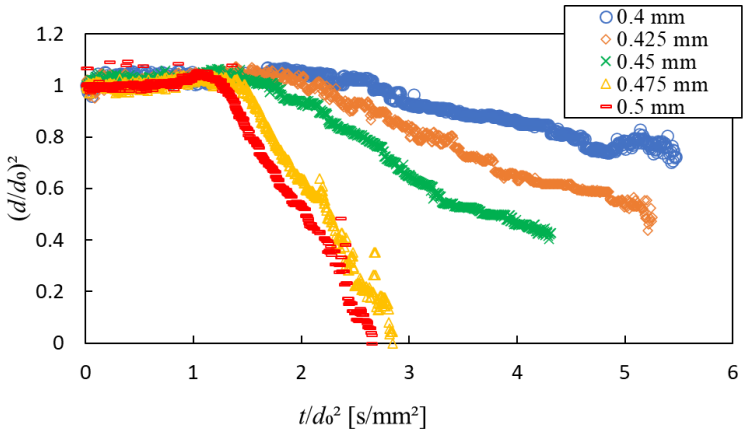

Fig. 4 Temporal variations of the squared diameter of Droplet L for different initial droplet diameters.

3.2 Temperature Distribution around Droplet L

Under the condition that the hot flame did not appear around Droplet L, we measured the temperature distribution of Fiber A defined in Fig. 1 with TFP method. Figure 5 shows the temperature distributions around Droplet L for $d_0 = 0.45$ mm at different times. The horizontal axis is the normalized position x/d_0 relative to the center of Droplet L, and the vertical axis is temperature. Figure 5(a) shows the process of cool flame development. At $t/{d_0}^2 = 1.11$ s/mm², the temperature is slightly higher around Droplet L. It is probably caused by light emission from igniter and burning Cluster H. At $t/{d_0}^2 = 1.48$ s/mm², the temperature around Droplet L is higher than that at $t/{d_0}^2 = 1.11$ s/mm². Especially on the

left side of Droplet L, the temperature reaches about 750 K. So, it seems that a cool flame occurred. After that, the cool flame continues to develop until $t/{d_0}^2 = 1.85$ s/mm², when the temperature around Droplet L shows the maximum value.

Figure 5(b) shows the process of the cool flame extinction. At $t/{d_0}^2 = 1.98$ s/mm², the temperature gradient on the left side of Droplet L is caused by burning of Cluster H. However, it gradually disappears toward 2.04 s/mm². Therefore, the cool flame could not be maintained because the heat supply from Cluster H to Droplet L was cut off.

Figure 6 shows that the relationship between the state of vaporization of Droplet L and the temperature distribution at specific times for d_0=0.45 mm. The red line in the left-hand side graph is the approximation line to calculate the vaporization-rate constant. The graph on the upper right of Fig. 6 is the temperature distribution when the cool flame just occurred, and the graph on the lower right of the figure is the temperature distribution when the cool flame just disappeared. Therefore, the cool flame appeared from the start of vaporization of Droplet L until about $t/{d_0}^2 = 2.04$ s/mm². The vaporization-rate constant for this period is 0.28 mm²/s. This value is close to the value reported by Ref. 6)

Figure 7 shows that the relationship between the state of vaporization of Droplet L and the temperature distribution at a specific time for $d_0 = 0.425$ mm. At this time, there is no high temperature region around Droplet L. So, the cool flame did not occur. Droplet L vaporized due to thermal effect of burning Cluster H. For $d_0 = 0.4$ mm, the same tendency was seen.

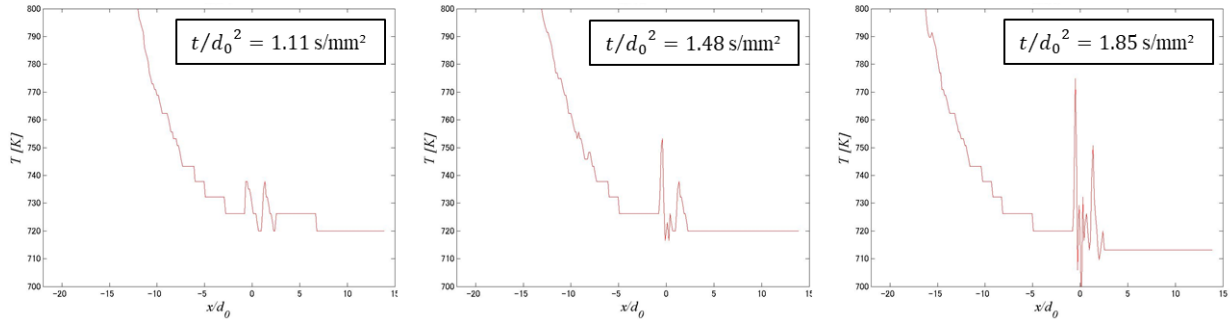

(a) Development of a cool flame.

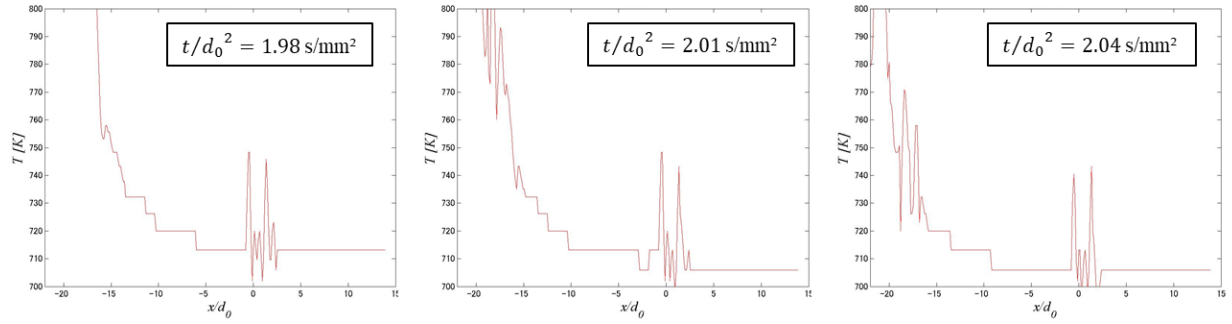

(b) Extinction of a cool flame.

Fig.5 Temperature distribution around Droplet L (x/d_0=0) at different times in $d_0 = 0.45$ mm.

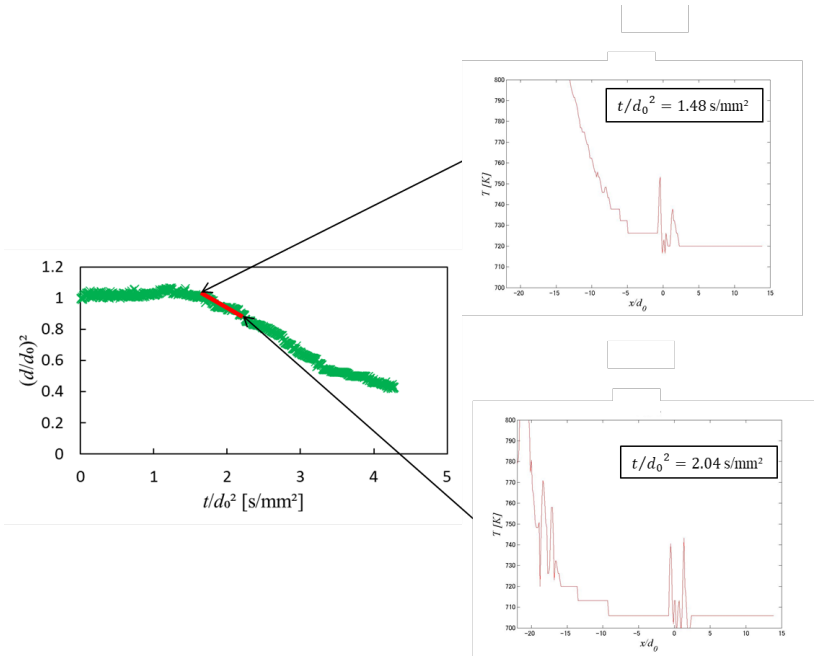

Fig. 6 Temporal variation of the squared diameter of Droplet L and temperature distributions for $d_0 = 0.45$ mm.

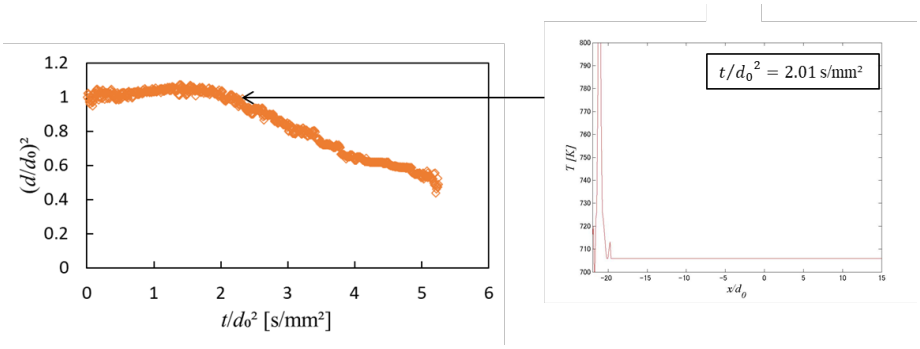

Fig. 7 Temporal variation of the squared diameter of Droplet L and temperature distribution for $d_0 = 0.425$ mm

4. Conclusion

We investigated the occurrence of a cool flame during flame spread over droplet-cloud elements at atmospheric pressure in microgravity. The main conclusions are as follows:

(1) It is difficult to judge the occurrence of the cool flame only by vaporization-rate constant. The temperature distribution measurement is helpful to identify the cool flame.
(2) The vaporization-rate constant with the cool flame is 0.28 mm²/s.
(3) The cool flame disappears just after the heat supply is cut off.

Acknowledgments

This research was subsidized by JSPS KAKENHI Grant-in-Aid for Scientific Research (B) (18H01625). The authors wish to thank Ms. Y. Hara for her help in experiments.

References

1) M. Mikami, M. Kikuchi, Y. Kan, T. Seo, H. Nomura, Y. Suganuma, O. Moriue, and D. L. Dietrich: International Journal of Microgravity Science and Application, **33(2)** (2016) 330208.
2) Y. Yoshida, K. Iwai, K. Nagata, T. Seo, M. Mikami, O. Moriue, T. Sakashita, M. Kikuchi, T. Suzuki, and M. Nokura: Proceedings of the Combustion Institute, **37(3)** (2019) 3409.
3) M. Mikami, H. Nomura, Y. Suganuma, M. Kikuchi, T. Suzuki, and M. Nokura: International Journal of Microgravity Science and Application, **35(2)** (2018) 350202.

4) M. Mikami, Y. Yoshida, T. Seo, T. Sakashita, M. Kikuchi, T. Suzuki, and M. Nokura: Microgravity Science and Technology, **30(4)** (2018) 535.
5) M. Mikami, Y. Yoshida, M. Kikuchi, and D. L. Dietrich: 12th Asia-Pacific Conference on Combustion, (July. 1.-5. 2019) Paper No. ASPACC2019-1504.
6) K. Matsumoto, Y. Yoshida, M. Mikami, and M. Kikuchi: 29th European Conference on Liquid Atomization and Spray Systems, (Sep. 2-4 2019) paper No. ilass19:247373
7) M. Mikami, K. Matsumoto, Y. Yoshida, M. Kikuchi, and D. L. Dietrich: Proc. Combust. Inst., 38, (2021), in press.
8) V. Nayagam, D. L. Dietrich, P. V. Ferkul, M. C. Hicks, and F. A. Williams: Combustion and Flame **159 (12)** (2012) 3583.
9) V. Nayagam, D. L. Dietrich, M. C. Hicks, and F. A. Williams: Combustion and Flame, **162(5)** (2015) 2140.